Chemical Geology, 107 (1993) 111–131
Elsevier Science Publishers B.V., Amsterdam

[AL]

Vegetation-induced, subsurface precipitation of carbonate as an aggradational process in the permanent swamps of the Okavango (delta) fan, Botswana

T.S. McCarthy[a], W.N. Ellery[b] and Karen Ellery[b]
[a]*Department of Geology, University of the Witwatersrand, P.O. Wits, Johannesburg 2050, South Africa*
[b]*Department of Botany, University of the Witwatersrand, P.O. Wits, Johannesburg 2050, South Africa*

(Accepted for publication February 26, 1993)

ABSTRACT

Islands constitute an important geomorphological component of the permanent swamps of the Okavango alluvial fan. Studies of the topography, soil chemistry, groundwater chemistry and vegetation cover across several islands indicate that many islands form as a result of the subsurface precipitation of calcite and probably amorphous silica, which produces vertical expansion, creating topographic relief. The main agent responsible for this precipitation is transpiration, especially by large, deep-rooted trees, which increases the salinity of the groundwater, leading to saturation in calcite and silica. The process ultimately leads to the development of highly saline groundwater and results in marked zonation of vegetation across the islands. Numerical modelling of the process suggests that salinization of the groundwater beneath an island takes between 100 and 200 yr. High calcite contents in island soils appear to be the product of several cycles of salinization, which are interspersed with periods of swamp abandonment during which the more soluble alkali salts are leached from the islands. Island formation represents an important process in the overall aggradation of the alluvial fan.

1. Introduction

The Okavango Delta alluvial fan of northern Botswana (Fig. 1) covers an area of ~22,000 km^2 and is amongst the largest alluvial fans on Earth. It has a remarkably low average gradient (1:3600) and ~6000 km^2 are covered by perennial swamps. Water and sediment are distributed across the fan surface by meandering and anastomosing channels which are flanked by extensive swamps. The positions of the channels and hence the distribution of water and sediment on the fan are constantly changing, due mainly to channel avulsion, leading to the fairly even distribution of sediment across the upper, permanently flooded portion of the fan (McCarthy et al., 1988, 1991a).

Islands, ranging in size from a few square metres to several hectares, occur scattered throughout the permanent swamps. These constitute between 10% and 20% of the area of the permanent swamps and are clearly aggradational features. Hence, islands form an important component of the architecture of the fan. Most of the islands are of irregular shape and their mode of formation is enigmatic. Limited studies carried out on islands suggest that they represent sites of subsurface accumulation of silica and calcite, possibly brought about by capillary evaporation or by transpiration (McCarthy and Metcalfe, 1990; McCarthy et al., 1991b).

In view of the importance of island-forming processes in shaping the overall morphology of the fan, further detailed studies were carried out on several islands in the permanent swamps. The purpose of the study was to investigate the possible influences of soil chem-

009-2541/93/$06.00

istry, groundwater chemistry and vegetation cover on the morphology of islands.

2. The Okavango Delta

The Okavango Delta fan lies within grabens at the southern extremity of the East African rift system (Scholtz, 1975; Hutchins et al., 1976). It represents the terminal depository for the Okavango River system which drains central Angola, as all of the sediment transported by the river is deposited on the fan. The Delta is situated in the semi-arid Kalahari Desert, where evapotranspiration exceeds precipitation by a factor of 3 and ~96% of the annual discharge of the Okavango River is lost to the atmosphere on the fan (Dinçer et al., 1981). It is divided into three distinct physiographic regions (Wilson, 1973): (1) the upper Panhandle region, characterized by meandering chan-

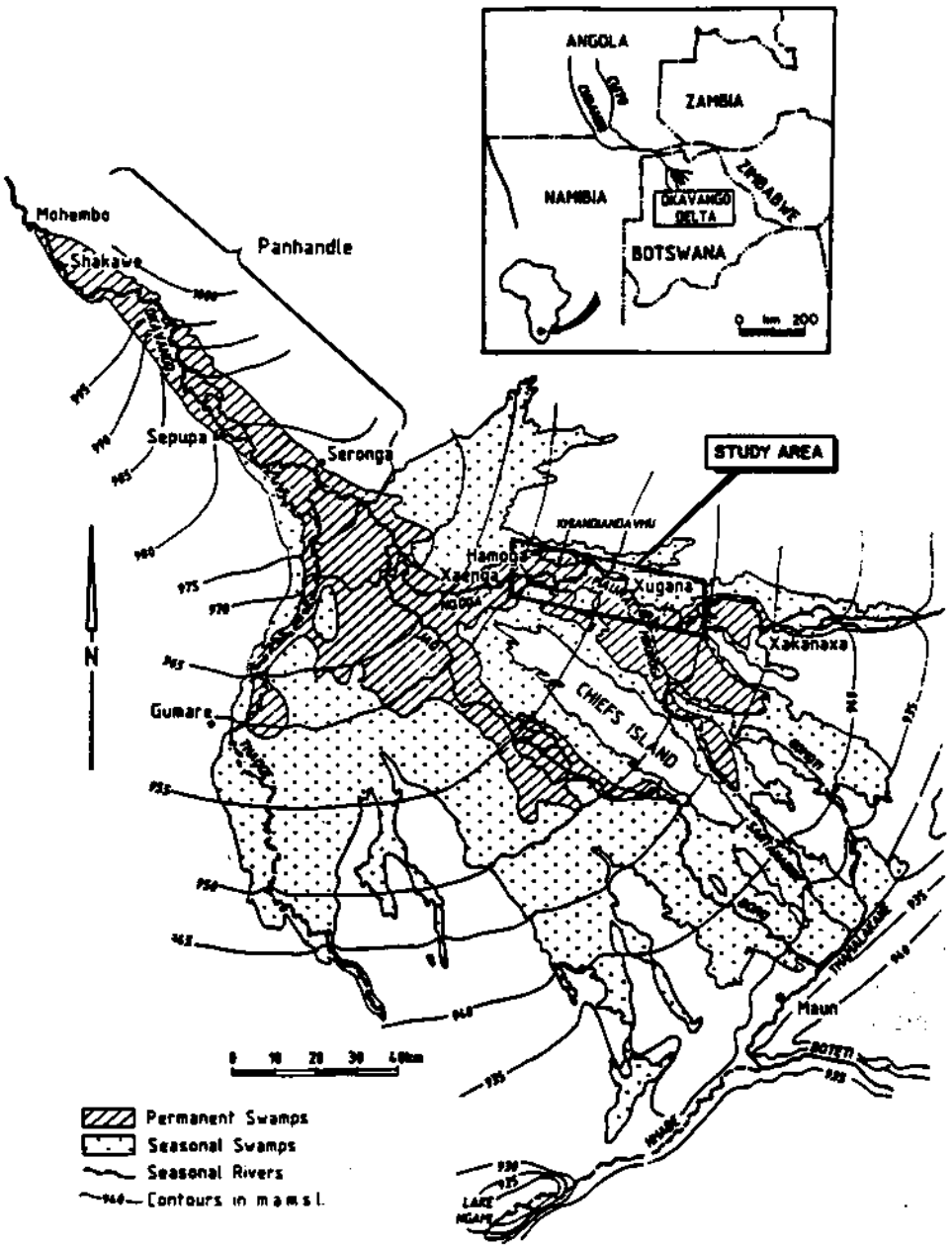

Fig. 1. The Okavango Delta

nels flanked by permanent swamps and laterally confined by what appear to be eroded fault scarps; (2) a region of perennial swamps around the apex of the fan; and (3) the lower seasonal swamps or floodplain (Fig. 1).

The perennial swamps are dominated by the giant sedge *Cyperus papyrus* and the grass *Miscanthus junceus*. Isolated channel systems distribute water through the perennial swamps, although a considerable proportion of water flows outside of the channels in the heavily vegetated swamps (McCarthy et al., 1991a). The major channel system at present is the Nqoga–Maunachira system in the northeastern region of the swamps, but channel systems are subject to avulsion and abandonment and major shifts in water distribution have occurred in historical times (Wilson, 1973; Shaw, 1984; McCarthy et al., 1988). Average water depth in the swamps is 1.5 m (UNDP, 1977), but may exceed 5 m near channels (McCarthy et al., 1991a).

Islands are an important component of the permanent swamps. They vary considerably in size and shape and invariably support the growth of large trees. The extent of tree cover is variable with some islands having complete tree cover, while others support only a narrow fringe zone of trees, the centre of the island then being devoid of all woody vegetation and the soil surface covered by a thin efflorescent crust of trona (McCarthy et al., 1986b, 1991b; McCarthy and Metcalfe, 1990). Some islands contain small saline pans (McCarthy et al., 1991b). Islands seldom rise more than a metre above the water level of the surrounding swamps, except for the occasional termitarium.

3. Study methods

Six islands on the Nqoga–Maunachira channel-swamp system were selected for this study (Fig. 2). Five of these islands are small, oval- to irregular-shaped features, while the sixth (island *E*), is a long, sinuous island, probably representing a former channel bed, now raised

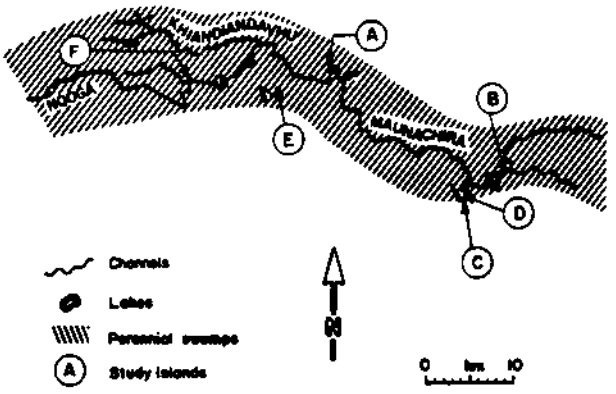

Fig. 2. Location of the islands chosen for study.

as a result of topographic inversion (McCarthy et al., 1986a, 1988). Vegetation cover on these islands varies from a narrow fringe of trees (island *F*) to heavily vegetated (island *E*). The field work was carried out during October 1990, towards the end of the long dry season.

A single transect was measured across the minor diameter of each island. Topographic elevation was measured along the transect using a Kern® level. Auger holes were made at ~20-m intervals to a depth of ~1.4 m and soil samples were collected at ~20-cm intervals in each auger hole. Groundwater level was allowed to equilibrate in the auger holes and the water level elevation recorded. Water samples were collected for analysis from each of the auger holes and the electrical conductivity measured using a Hanna® conductivity meter. Vegetation was also recorded along the transects using an estimate of cover-abundance described by Mueller-Dombois and Ellenberg (1974). The cover scores of *1*, *2*, *3*, *4*, *5*, *6*, *7* and *8* were assigned to intervals between 0%, 1%, 2%, 5%, 10%, 25%, 50%, 75% and 100%, respectively.

Soil samples were milled to −200 mesh and were analysed for CaO, MgO and Na_2O by X-ray fluorescence spectrometry (XRF) on undiluted powder briquettes. Ten of the soil samples showing a range of the oxide abundances were analysed by XRF using the fusion method of Norrish and Hutton (1969), and these

served as standards for the analysis of the remaining samples. This approach was used to ensure that standards and samples had very similar compositions, thus avoiding matrix correction problems which arise with powder briquette XRF methods. Analytical precision is of the order of ±15% (relative) which is considered adequate for the purpose of the present study. Water samples were analysed by the South African Bureau of Standards using the techniques described by McCarthy et al. (1991b).

4. Results and discussion

4.1. Topographic profiles

Topographic relief of the islands is low, the maximum topographic height being 120 cm above swamp water level (Figs. 3–8). Topographic profiles are irregular (island *E*), domical (island *C*) or may show two domes (islands *A* and *D*). In plan, these last-mentioned types typically have a raised mound around the entire island, with a central depression in which a pan sometimes develops (e.g., island *D*).

4.2. Water table beneath the island

In all the islands studied, the water table beneath the island is drawn down below the level of the surrounding swamp water, typically by ~20 cm (Figs. 4–8), but in the case of island *A* by as much as 50 cm (Fig. 3). This implies that water is being lost from the islands at a rate sufficient to create an hydraulic head relative to the surrounding swamp. Evaporation from the capillary fringe of the centrally located pans could be partly responsible, as suggested by McCarthy and Metcalfe (1990). However, it seems more likely that transpiration by deep-rooted trees fringing the islands is mainly responsible for lowering the water table beneath the islands, particularly as the water table gradients are generally steepest near the edges of the islands where the deep-rooted

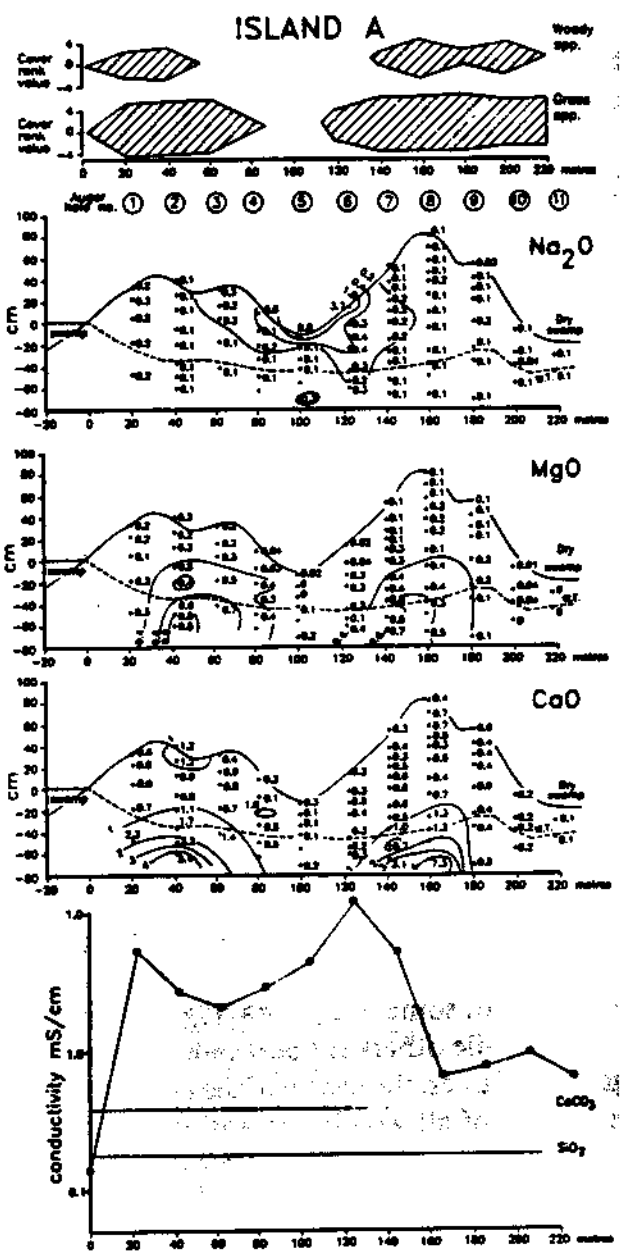

Fig. 3. Profiles across island *A* showing: (a) vegetation cover; (b) soil Na_2O; (c) soil MgO; (d) soil CaO; and (e) electrical conductivity of groundwater: the conductivities at which calcite and amorphous silica saturate are indicated (see text for details).

woody vegetation is most dense, and where capillary evaporation would be most suppressed.

4.3. Soil chemistry

X-ray diffraction, SEM, optical microscopic and chemical studies carried out on island soils

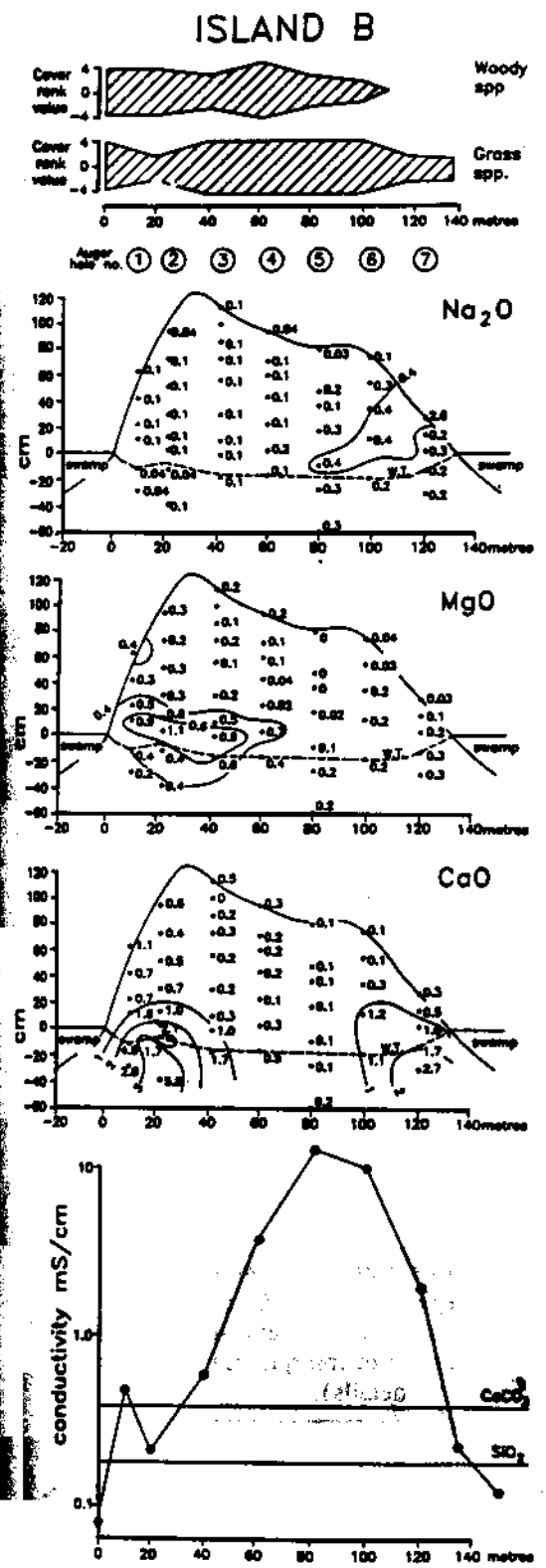

Fig. 4. Profiles across island *B* showing: (a) vegetation cover; (b) soil Na_2O; (c) soil MgO; (d) soil CaO; and (e) electrical conductivity of groundwater: the conductivities at which calcite and amorphous silica saturate are indicated (see text for details).

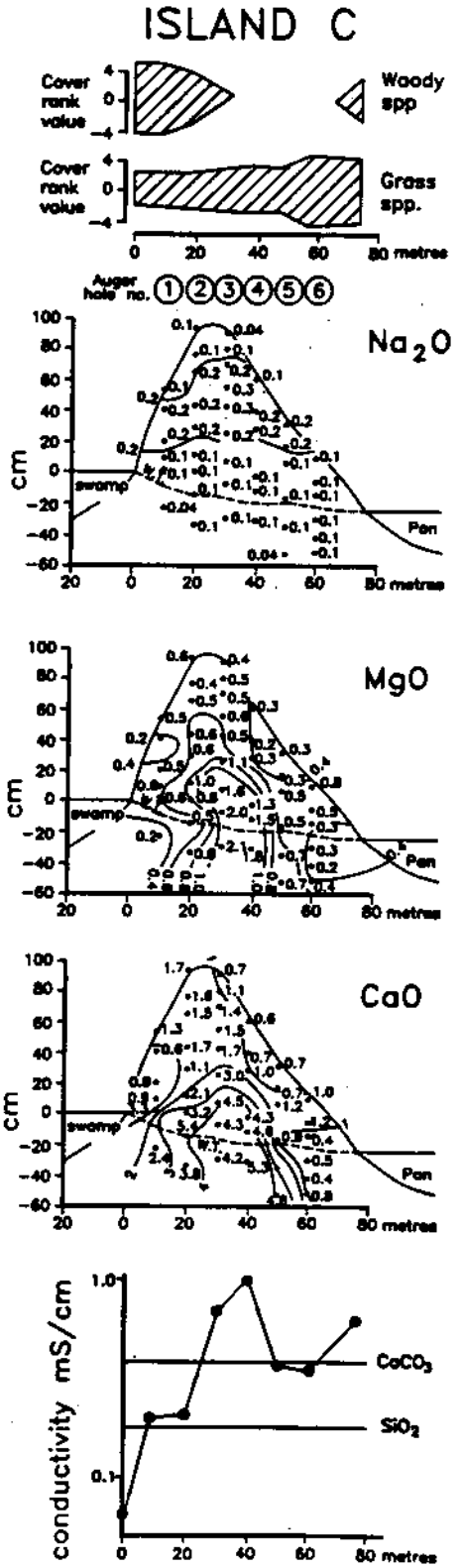

Fig. 5. Profiles across island *C* showing: (a) vegetation cover; (b) soil Na_2O; (c) soil MgO; (d) soil CaO; and (e) electrical conductivity of groundwater: the conductivities at which calcite and amorphous silica saturate are indicated (see text for details).

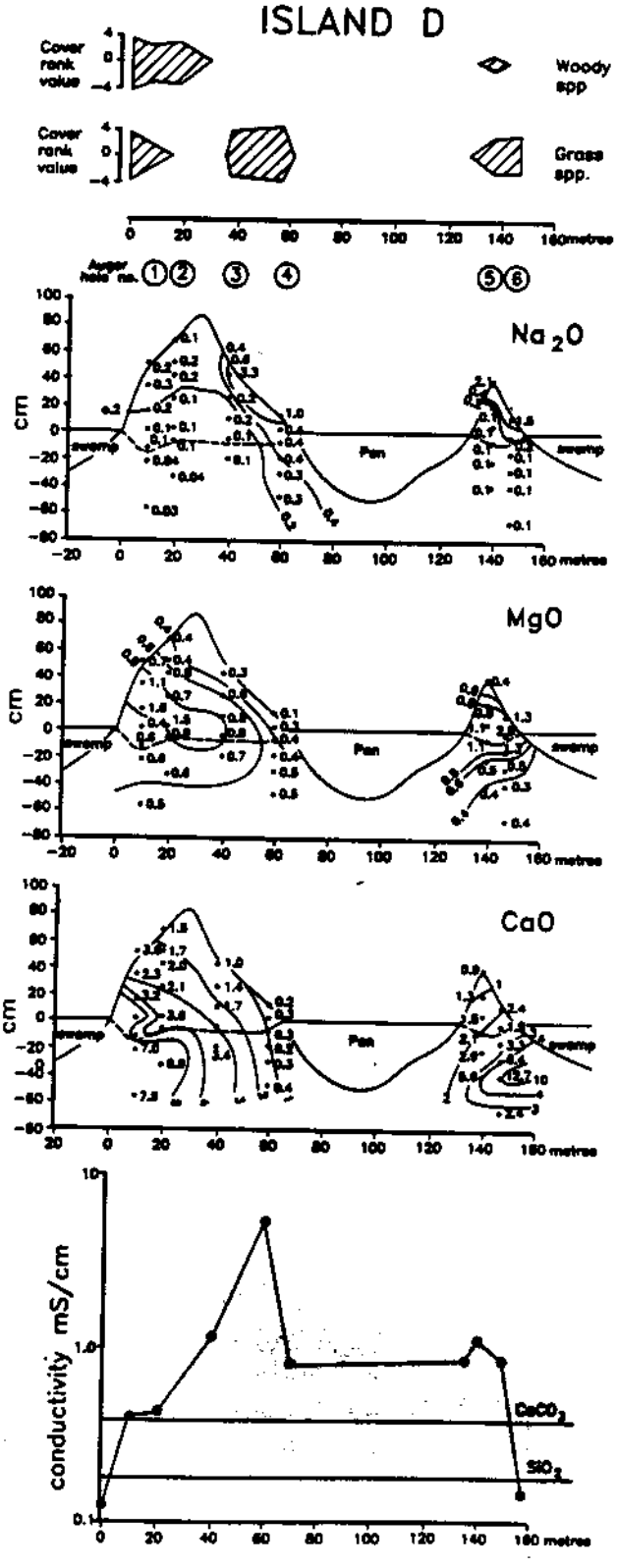

Fig. 6. Profiles across island *D* showing: (a) vegetation cover; (b) soil Na_2O; (c) soil MgO; (d) soil CaO; and (e) electrical conductivity of groundwater: the conductivities at which calcite and amorphous silica saturate are indicated (see text for details).

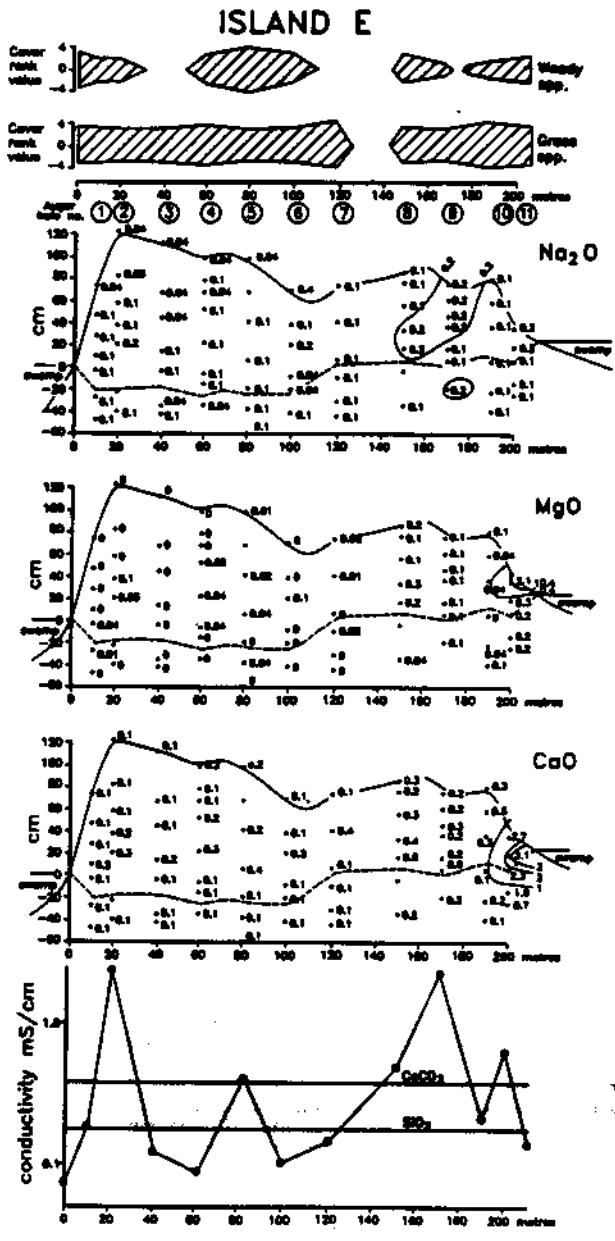

Fig. 7. Profiles across island *E* showing: (a) vegetation cover; (b) soil Na_2O; (c) soil MgO; (d) soil CaO; and (e) electrical conductivity of groundwater: the conductivities at which calcite and amorphous silica saturate are indicated (see text for details).

by McCarthy et al. (1986b, 1991b) and McCarthy and Metcalfe (1990) indicate that they consist predominantly of fine sand (average grain diameter 0.2 mm) in a matrix of very fine calcite, kaolinite, amorphous silica and minor K-feldspar. Locally, surface efflorescent crusts of trona with minor thermonatrite also occur.

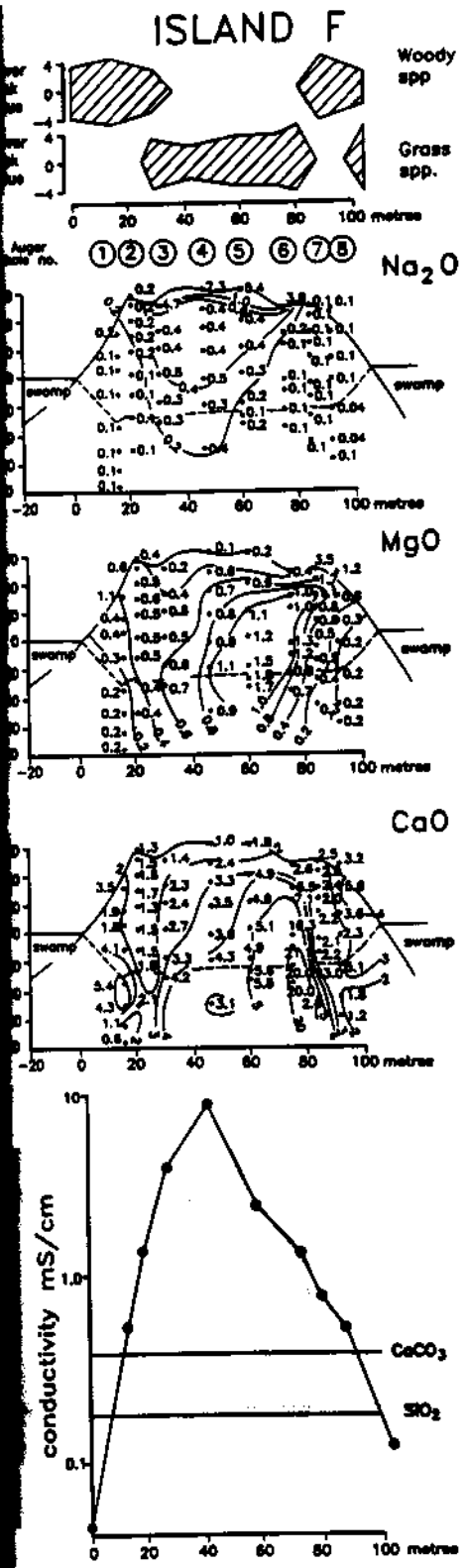

Fig. 8. Profiles across island *F* showing: (a) vegetation cover; (b) soil Na_2O; (c) soil MgO; (d) soil CaO; and (e) electrical conductivity of groundwater: the conductivities at which calcite and amorphous silica saturate are indicated (see text for details).

The concentration of CaO, MgO and Na_2O in island soils, which reflect the abundances of magnesian calcite and trona, are shown in Figs. 3–8. Sampling depth was limited to 1.4 m so that the nature of the deep soils could not be determined. Nevertheless, very significant variations in the abundances of these components are evident. All of the islands exhibit enrichment in CaO and MgO with depth, in most cases showing concentration maxima towards the edges of the islands, but in the case of the narrowest island (*C*), forming only a single maximum beneath the centre of the island (Fig. 5). The highest concentrations of CaO occur just below the water table. In contrast, maximum Na_2O abundance generally occurs at the surface of the island, usually above the central part where subsurface CaO is low (e.g., island *A*).

There is a close correspondence between the CaO and MgO abundances in the subsurface and the topography of the islands, except in the case of island *E* (Figs. 3–8), with elevated concentrations of CaO and MgO corresponding with topographic highs. Wider islands tend to have two distinct concentration maxima (islands *A*, *D*, *F*), while the narrowest island (*C*) has only a single maximum. There is a slight difference in the positions of the concentration maxima for MgO and CaO. Where two CaO maxima are present, the corresponding MgO maxima are usually displaced towards the centre of the island and to a slightly higher elevation compared to the CaO maxima. The magnitudes of the CaO maxima vary from >20% in island *F* to 3% in island *E*. There is no obvious relationship between height above water level and the maximum CaO abundance when all islands are considered.

4.4. Groundwater chemistry

Chemical analyses of groundwater samples are listed in Table 1. The water is bicarbonate dominated, a characteristic feature of continental areas (Garrels and MacKenzie, 1967).

TABLE 1

Chemical analyses of swamp- and groundwater (conductivity in mS cm^{-1}; concentrations in mg l^{-1})

Sample	pH	Conductivity	Ca	Mg	Na	K	SiO_2	Cl^-	SO_4^{2-}	CO_3^{2-}	HCO_3^-
A swamp	6.5	0.138	5	1	9	4	15	<5	<5	0	32
A_1	8.0	5.1	19	30	1,650	223	130	13	<5	379	3,994
A_4	8.6	2.8	25	32	660	192	100	–	–	400	1,273
A_6	9.0	11.8	5	5	4,100	960	45	–	–	2,331	6,572
A_7	7.8	4.0	72	99	650	452	110	200	<5	–	–
A_9	7.4	0.741	26	15	160	59	130	<5	<5	51	556
B swamp	6.3	0.076	7	2	9	5	19	–	–	0	42
B_1	7.1	0.223	84	6	15	9	81	–	–	11	239
B_3	8.0	3.8	24	128	2,300	438	110	–	–	569	5,700
B_4	8.6	13.8	10	9	5,200	1,070	65	–	–	2,362	9,605
B5	8.6	10.4	5	10	4,000	496	80	62	8	3,263	4,834
B_7	6.8	0.225	14	6	13	4	43	–	–	7	87
B_8	6.9	0.474	100	4	16	8	68	–	–	21	193
C swamp	6.9	0.064	5	1	6	4	10	–	–	0	32
C_1	7.0	0.203	60	4	13	7	71	–	–	15	166
C_3	7.1	0.726	56	32	125	34	120	–	–	112	367
C_4	7.8	1.02	16	16	160	196	120	–	–	37	712
C_6	7.1	0.36	56	22	13	42	110	–	–	31	224
C_7	7.4	0.63	88	36	75	38	62	–	–	90	297
D swamp	6.3	0.130	6	3	9	7	29	–	–	0	57
D_2	6.9	0.433	80	10	24	28	100	–	–	23	168
D_4	8.1	5.3	20	30	1,550	164	130	320	<5	497	2,812
D_5	7.1	1.02	72	10	200	10	110	–	–	90	379
D pan	7.8	0.77	24	16	185	50	100	–	–	131	360
E_4	6.2	0.090	6	1	22	7	34	–	–	–	–
E_6	6.1	0.101	14	3	14	5	51	–	–	3	76
E_8	6.5	0.478	52	7	49	19	86	–	–	24	233
E_{10}	6.2	0.204	23	6	21	7	92	–	–	14	128
E_{11}	6.8	0.608	116	19	52	9	68	–	–	47	177
E_{12}	6.9	0.133	21	3	12	8	47	–	–	6	102
$F1$	6.8	0.044	68	14	62	5	88	<5	<5	29	302
F_2	7.2	1.41	56	41	220	69	120	27	26	96	749
F_3	8.6	4.11	6	5	1,750	89	90	76	140	678	3,196
F_4	9.3	9.27	3	<1	4,200	314	88	320	560	2,610	5,182
F_5	8.5	2.50	8	18	700	52	100	–	–	177	1,501
F_9	8.9	0.386	4	1	1,500	75	79	–	–	942	2,013
F_{11}	5.7	0.120	3	<1	8	3	21	–	–	0	27

– = not determined.

Salinity is variable, spanning three orders of magnitude. In swamp water, the most abundant dissolved species is SiO_2 but this becomes less important with increasing salinity and in the more saline groundwaters, sodium bicarbonate dominates.

As the groundwater beneath islands is ultimately derived from swamp water, which is fairly uniform in composition throughout the study area, the chemical evolution of the groundwater beneath all of the islands in this study is conveniently discussed together. Chlo-

used as a conserved element chemical evolution of water. In the Okavango Delta, abundance levels of this ion are generally low, especially in swamp water, leading to large analytical uncertainties and in addition there are indications that Cl is not conserved in the groundwater (McCarthy et al., 1991b). Accordingly, Na is preferred as a conserved element although it can only be used if the water is not saturated in an Na-bearing mineral (Eugster, 1980). This is not a problem in the present study as none of the water samples approach saturation in sodium salts, which occurs in evaporated swamp water at a concentration of ~120,000 ppm Na when trona crystallizes (McCarthy et al., 1991b).

Figs. 9, 10 and 11 show plots of SiO_2, Ca and Mg, respectively, against Na in surface and groundwater. Included in these plots are analyses of swamp water reported by Hutton and Dinçer (1976) as well as unpublished analyses of channel and swamp water of the senior author and ground and surface water reported by McCarthy et al. (1991b). Distinct evolutionary trends are evident. With increasing Na concentration, the concentrations of SiO_2 increases up to an Na concentration of ~20 ppm, above which no further increase in SiO_2 occurs. This indicates saturation in and precipitation of a silica-bearing phase, but possibly under the influence of a buffer (Eugster and Jones, 1979; Eugster, 1980). In contrast, Ca concentration continues to increase with further increase in Na, until ~50 ppm Na, beyond which the concentration of Ca falls, indicating crystallization of a phase containing calcium. Mg shows a similar evolutionary trend to Ca, but peaks at a slightly higher Na concentration. The mineralogy of the soils indicates that SiO_2 precipitates mainly as amorphous silica, while Ca and Mg precipitate as magnesian calcite. It is evident from Figs. 9–11 that the groundwater from all of the islands defines a coherent evolutionary path, albeit with some scatter, and the Na content therefore forms a useful monitor of the state of evolution of the groundwater, particularly whether or not it is saturated in amorphous silica and calcite.

The Na concentration of the water is highly correlated with its electrical conductivity (Fig. 12), except at low Na concentrations, and therefore this simple field measurement also provides a monitor of the state of evolution of

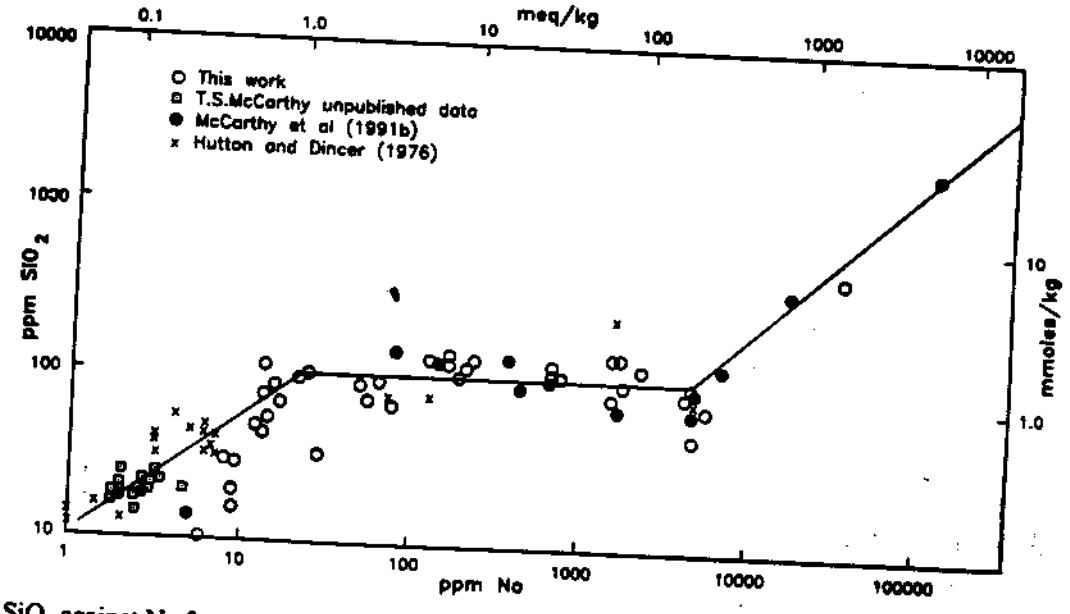

9. Plot of SiO_2 against Na for ground- and surface water of the Okavango Delta.

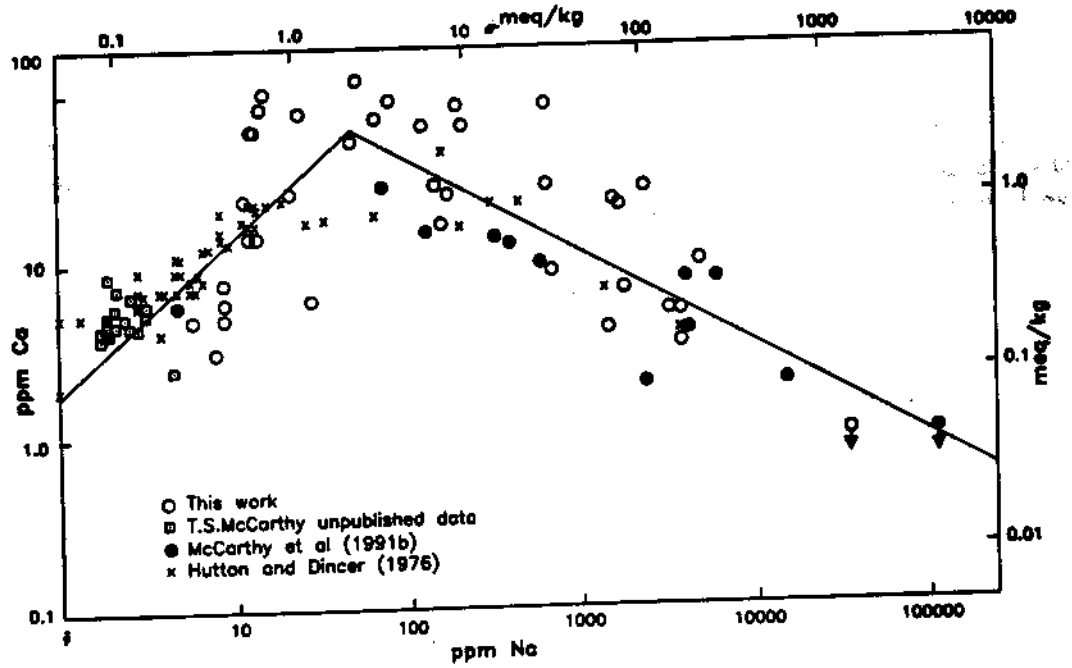

Fig. 10. Plot of Ca against Na for ground- and surface water of the Okavango Delta.

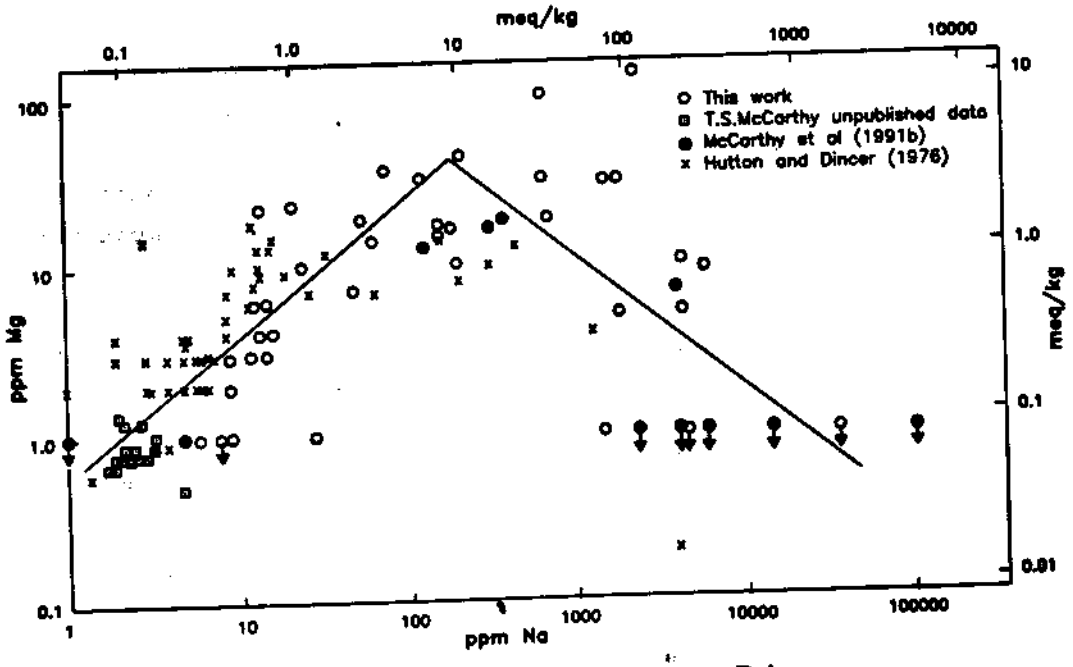

Fig. 11. Plot of Mg against Na for ground- and surface water of the Okavango Delta.

the groundwater. Saturation in amorphous silica occurs at a conductivity of ~0.18 mS cm^{-1} (Figs. 9 and 12), while saturation in calcite occurs at ~0.38 mS cm^{-1} (Figs. 9, 10 and 12).

The conductivity of the groundwater beneath each of the islands is shown in Figs. 3e–8e. In all cases, the salinity of the groundwater increases inwards from the low values in the surrounding swamp water, in some cases rising to a single maximum near the centre of the island (e.g., islands *B* and *F*), while in others more complex patterns are evident, as in is-

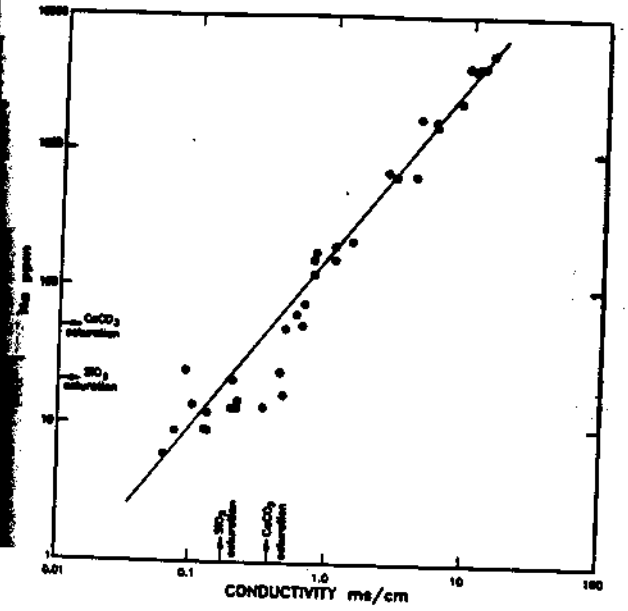

Fig. 12. Plot of Na against electrical conductivity for water samples collected during this study.

land *E*. Comparison of the conductivity plots with the corresponding distribution of CaO indicates that elevated CaO (i.e. high calcite content) occurs on the inside of points where the groundwater conductivity curve crosses the conductivity at which calcite saturates. In general, the highest soil CaO concentrations occur below the water table, although elevated concentrations also extend upwards into the capillary zone.

4.5. Distribution of vegetation

The distribution of woody and grass species along each of the transects is shown in Figs. 3a–8a. Grasses generally occur across the entire length of the transects although the abundances of individual species change. Exceptions occur where woody vegetation is dense or where soils are particularly saline. Woody species are often absent in the central sections of the transects.

The species composition of woody plant communities appears to be sensitive to groundwater chemistry. Fig. 13a illustrates the occurrence of the more common woody species in relation to groundwater conductivity. Certain species, notably *Diospyros mespiliformis*, *Syzygium cordatum*, *Ficus verruculosa*, *Phoenix reclinata* and *Ficus sycamorus* occur where groundwater conductivity is low, while other species show a wider range of tolerance. Relatively few species occur where conductivity exceeds 6 mS cm^{-1}. Grass species, being shallower rooted, are affected by increases in salinity in the soils. Fig. 13b illustrates the occurrence of grasses in relation to the Na con-

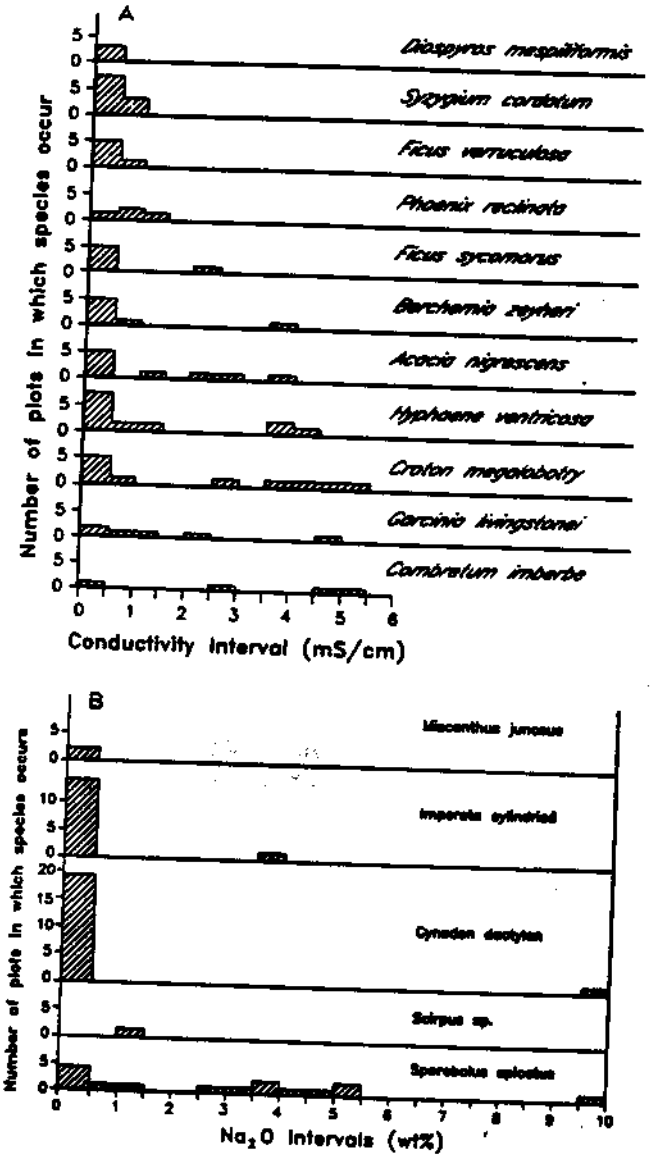

Fig. 13. a. The occurrence of major woody species in relation to groundwater conductivity.
b. The occurrence of grasses in relation to the Na content of surface soil.

tent of the surface soils. *Miscanthus junceus* is an aquatic species and is confined to island fringes. *Imperata cylindrica* and *Cynodon dactylon* generally occur in the less saline soils while *Sporobolus spicatus* is able to tolerate a wide range of soil salinity.

It is evident from the data presented in Fig. 13 that plant communities tend to be most diverse around the fringes of the islands where the groundwater and soil salinities are low. Towards the interior, diversity decreases, woody species thin out and eventually disappear leaving only the grass species *S. spicatus*. Under extreme salinity, this grass also disappears, leaving barren, trona-encrusted soil (e.g., island *A*).

4.6. The link between vegetation, topography, the water table and groundwater chemistry

As shown previously, most of the island fringes are heavily vegetated and transpiration by deep-rooted woody plants lowers the water table beneath the island. The water table profile must therefore represent a steady-state condition between transpirational loss and replenishment of groundwater from the surrounding swamp. It is likely that the extent of drawdown of the water table will vary seasonally since transpiration rate varies seasonally. In addition, swamp water level is also subject to seasonal fluctuations, although in the case of the area studied, this is generally < 20 cm.

During transpiration, plants remove mainly water and actively exclude dissolved solutes other than those required to meet physiological needs. Consequently, the salinity of the groundwater is increased by transpiration, leading eventually to saturation in amorphous silica and calcite, which precipitate in the soils. McCarthy and Metcalfe (1990) have demonstrated that precipitation of these minerals in the soil will lead to significant volume expansion. Such expansion is probably the cause of the correspondence between CaO content of soils and the topography of the islands. It should be noted that amorphous silica contents were not determined in this study but it is evident from the compositions of swamp water (Table 1) that the quantity of such silica will approximately equal that of magnesian calcite. Thus, the precipitation of amorphous silica from the groundwater must also play a very significant role in shaping the topography of islands.

4.7. Numerical modelling of groundwater flow beneath islands

The conductivity of the groundwater beneath the islands rises from the margins inwards. This suggests some lateral flow of groundwater, which may also account for the higher calcite concentrations towards the edges of the islands. In order to investigate this in more detail, a simple one-dimensional numerical model was developed which simulates evapotranspiration from an island. The model was written in FORTRAN to run on a mainframe computer.

For the purposes of the model, the island was assumed to be bilaterally symmetrical and only one-half was modelled. A discretized approach was adopted, the half-island being arbitrarily divided into twenty cells. An infinite reservoir of swamp water was assumed to exist to the left and below the half-island. The program was written to operate in increments of evapotranspiration and at each increment a fixed quantity of water (50 mm) was removed from each of the cells, leaving all solutes behind. The lost water was replaced by addition of water from the reservoir below (which has the composition of swamp water) and from the cell immediately to the left. In the left-most cell, water was added from below and from the swamp. After the water loss had been restored in all of the cells, the concentrations of Ca and Na were calculated and the cell tested for calcite saturation. The basis for the saturation test is empirical. On the plot of Ca vs. Na (Fig. 10), two linear branches are evident, to which lines were fitted and the equations determined. Below a

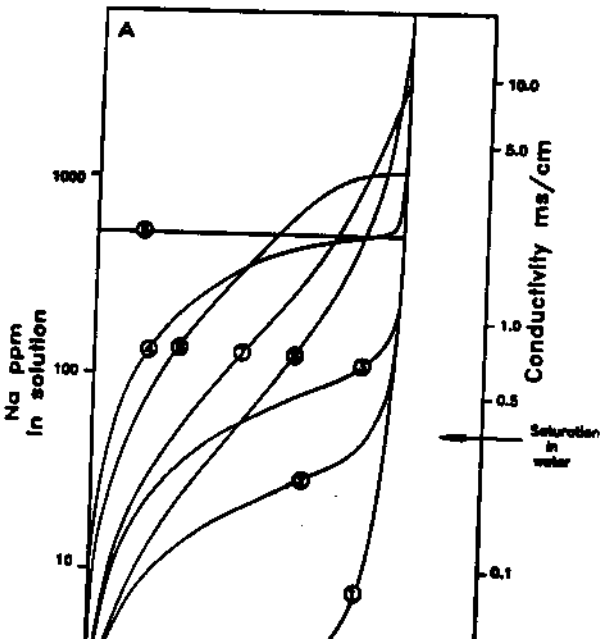

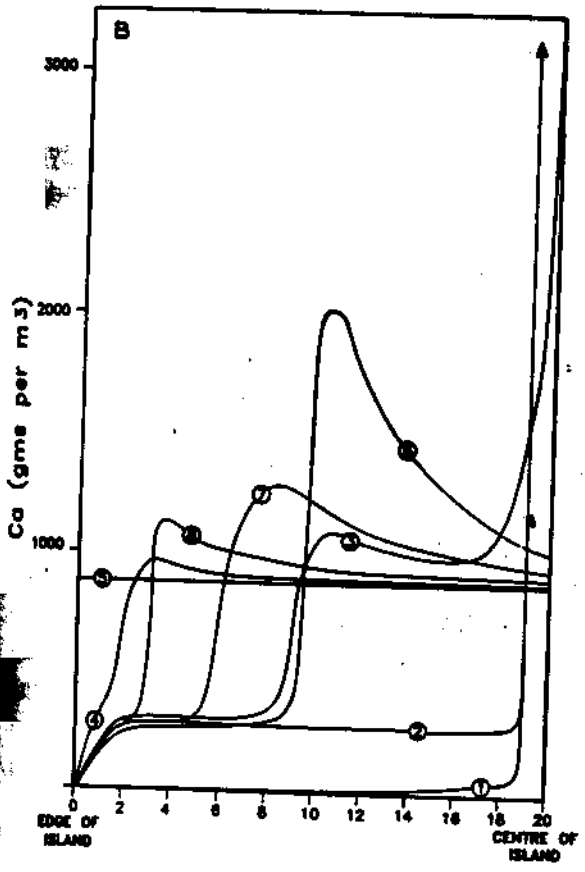

concentration of 49 ppm Na, Ca increases wit increasing Na and the water is not saturated i calcite, but the slope is less than unity indica ing that some Ca is being removed, probabl to serve the physiological needs of the plants Above 49 ppm Na, the groundwater is satu rated in calcite and precipitation will occur.

After the Ca and Na concentrations in a cel were calculated, the appropriate equation wa used to determine what the Ca content of th water in that cell should be. This was then compared to the calculated Ca, and an appro priate amount of Ca was removed as a precip itate. A running total of precipitated Ca was kept for each cell. Because of the empirical na ture of this method, it makes allowance for both Ca accumulated by plants as well as inorgani cally precipitated calcite.

The only independent variable in this model is the ratio of water input from below to that input from the cell to the left, which is, in ef fect, the groundwater flow pattern beneath the island. The strategy used was to vary this ratio and examine the effect on the Na content of the water and the accumulated Ca across the half-island. Two types of models were chosen:

Fig. 14. a. Results of a one-dimensional numerical model of evapotranspiration from one-half of an island. The curves illustrate the modelled Na concentration profiles in the groundwater beneath the half-island, showing the effect of varying the proportions of water input from below and from the left-hand side (see text for details). The conductivity scale is based on the linear relationship of Fig. 12. Model *1*: all water from the left in all cells. Model *2*: 50% water from below, 50% for left in all cells. Model *3*: 75% water from below, 25% from left in all cells. Model *4*: 95% water from below, 5% from left in all cells. Model *5*: all water from below. Model *6*: 50% water from below, 50% from the left for the left most cell, changing linearly to all water from below in the extreme right-hand side cell. Model *7*: 75% water from below, 25% from the left for the left most cell, changing linearly to all water from below in the extreme right-hand cell. Model *8*: 90% water from below, 10% from the left for the left most cell, changing linearly to all water from below in the extreme right-hand cell. The results shown each represent 5000 evapotranspiration increments, equivalent to 250 m of evapotranspiration. b. Accumulated Ca across the half-island for the models shown in (a).

one set involved a constant ratio of input from below and from the left (models *1–5*, Fig. 14); the other set involved a linear change in the proportion of water from the left across the half-island (models *6–8*, Fig. 14). Details of the models are provided in the caption to Fig. 14. The results illustrated in Fig. 14a show the concentration profiles after 5000 increments of evapotranspiration per cell, which, as will become evident later (p.125), is a sufficient number of cycles to establish steady state over all but the last few right-hand cells in most of the models.

Model *1* illustrates the resulting profile when all water is supplied from the left, i.e. only from the swamp adjacent to the island. This profile is clearly very different from the observed profiles, implying that simple lateral flow of groundwater does not occur. Model *5* represents the case where all the water is supplied from below (this model does not attain steady state), which is also different from the observed profiles. The remaining models represent intermediate cases with water input from below and from the left. These constant proportion models generally produce Na concentration profiles which are steep near the edge of the island, flattening towards the centre, but then rising sharply at the right-hand edge. The second group of models (variable input) produce steeper Na gradients overall and lack the sharp spike in the right-hand end cell. These latter models also all show a region of high Ca towards the edge of the island (Fig. 14b). This Ca peak moves towards the edge of the island (but decreases in size) as the proportion of water entering from the left is decreased. This is caused by the steepening of the concentration gradient at the edge of the island, which causes the saturation point of calcite to move closer to the island edge. The small plateau in Ca towards the edge of the island evident in some of the models represents biologically fixed Ca.

Of the six islands studied, four show distinct zones of Ca enrichment between the centre and margin and also show a concave-up pattern i each half of their conductivity profiles. Bot features are compatible with variable inpu models and suggest that lateral water flow i important near the edge of the islands albe only a small proportion of input, while to wards the centre, replenishment is largely fron below.

In many of the islands, the MgO maximum is displaced towards the centre of the islan compared to the CaO maximum. Eugster an Jones (1979) have noted that early formed calcite is low in MgO, crystallization of which increases the Mg/Ca ratio of the water, result ing in calcite of higher MgO. The lateral offse of MgO and CaO maxima is therefore also in dicative of lateral flow. In very narrow islands the two marginal peaks in CaO and MgO may merge to form a single, central concentration maximum, as in island *C*.

The numerical model is one dimensional, and provides no information regarding the vertical distribution of Ca in the soils. All of the variable input models imply that there should be a zone of accumulation of Ca in the soils beneath the centre of the island although the zone of maximum Ca accumulation is towards the margin (Fig. 14b). Such centrally located zones of Ca enrichment were not found during the present study but this may relate to the limited depth of the soil samples. The isopleths of Ca may well close beneath the islands, as indicated schematically in Fig. 15a, but below the sampling depth used in this study. Closure in this way is compatible with the general topography of the islands. However, the numerical models assume that the islands are underlain by low-salinity swamp water and hence the brines produced by transpiration develop as a lens beneath the island surface. If the deep groundwater is saline and saturated in calcite, then no zone of accumulation will occur beneath the centre of the island, and the closure of the CaO isopleths would probably be as shown in Fig. 15b. No data are presently available on the composi-

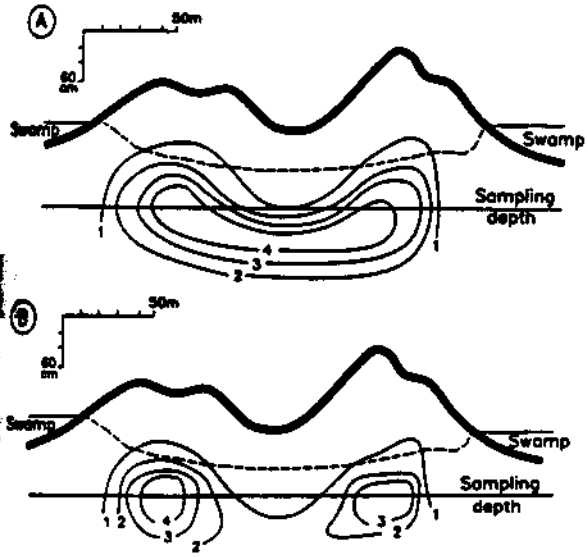

Fig. 15. Schematic diagrams showing possible closure of the CaO isopleths beneath an island: (a) assuming that the islands are underlain by water of the same composition as swamp water; and (b) assuming that the islands are underlain by groundwater which is saturated in calcite.

tional variations of groundwater with depth beneath islands in the Okavango Delta.

4.8. Time scales of salinization and carbonate precipitation beneath islands

Systematic aerial photography was first undertaken in the Okavango Delta in 1937, when oblique photographs were taken, and at various times since then vertical aerial photography has been carried out. Fig. 16 shows a series of aerial photographs of a cluster of islands (including island *F*) taken in 1937, 1969 and 1983. These photographs show a definite decrease in the vegetation cover of the island centres (especially of trees), and in the 1983 photographs the interiors of the islands are largely barren although they retain a fringe of dense vegetation. These islands were visited during the present study and the soils in the interior were found to be encrusted with a 2-cm-thick layer of trona. In the light of the data accumulated in this study, we can infer that the development of this crust and the destruction of the vegetation is the result of salinization of the groundwater and soils beneath the island (e.g., Fig. 13). On the islands shown in Fig. 16, this process was already well advanced by 1937, but increased significantly in the subsequent 46 years. This suggests that the process may be relatively rapid.

The numerical model described above can be used to investigate time scales of salinization. Each incremental step in the computation involves evapotranspiration of a fixed quantity of water (50 mm). The average evapotranspiration rate of the Delta is 1850 mm yr^{-1}, and assuming that this applies to the vegetated islands as well as open water, not an unreasonable assumption (Brown, 1981), incremental steps in the numerical model can be expressed in terms of time as shown in Fig. 17. It can be seen from this figure (which is based on model *8* of Fig. 14a) that as salinity in the groundwater beneath the centre of the island rises, a steady-state concentration profile develops towards the edge of the island and the groundwater beneath the fringe of the island always remains of low salinity. Hence, while conditions in the interior of the island evolve to a point where no vegetation can be supported, this does not occur around the fringes of the island. Comparison of the calculated salinity profiles with the profile measured beneath island *F* (Fig. 8e) indicates that the latter profile could have developed over a period of ~200 yr. This time scale seems compatible with the rate of disappearance of vegetation seen in the sequence of photographs in Fig. 16.

Several factors could cause the actual time scale of salinization to deviate from that determined from the numerical model. Although on average, transpiration rate from trees is approximately the same as open-water evaporation (Brown, 1981), transpirational losses from islands may initially exceed the average evapotranspirational loss for the Delta as a whole, because of the large leaf area index of vegetation on these islands. This would accelerate salinization. Furthermore, if the deep groundwater beneath islands is saline, salini-

zation would also be accelerated because most of the water which replaces transpirational loss comes from below. On the other hand, capillary evaporation (McCarthy and Metcalfe, 1990) may increase the time of salinization. This most likely occurs in the advanced stages of island evolution, when the interiors of islands are devegetated. In this process, saline groundwater is drawn up by capillarity and evaporates, depositing trona on the soil surface. Lower-salinity water from beneath the island is drawn in to replace the loss. As a consequence, Na does not accumulate in the groundwater to the extent indicated in the numerical model, but is transferred to the surface soil. Rainwater would dissolve the surface trona and return the salts to the groundwater, but because evapotranspiration exceeds precipitation by a factor of 3, there will be a net transfer of Na to the soil surface. The distribution of Na in the islands (e.g., island *A*) indicates that capillary evaporation is indeed an

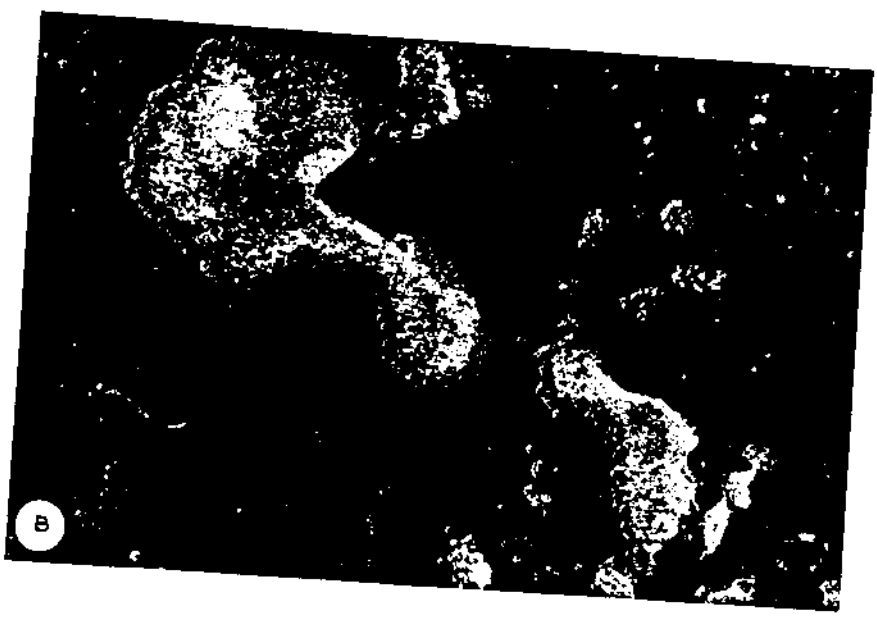

Fig. 16. Aerial photographs of a group of islands, including island *F*: (a) taken in 1937 (oblique photography); (b) 1969; and (c) 1983. Note the decline in vegetation density in the interior of the islands over the period of aerial photography. The dumbbell-shaped island is 1 km long

important process on the islands. This process could also account for the continued increase in salinity in the centres of islands after the vegetation has died off.

It is evident from the model calculations in Fig. 17 that the time scale required for salinization to occur assuming no transfer of Na to the soil is of the order of 100–200 yr. If transfer of Na to the soil is allowed for, this will increase. Over a period of 0.2 Myr, the quantity of calcite which could accumulate beneath the surface is very small, equivalent to ~1000 ppm CaO. This is 30–60 times smaller than is observed beneath the islands studied, except possibly in the case of island *E* which generally has low soil CaO concentration. This indicates that the time scale of accumulation of Na in the groundwater is between one and two orders of magnitude less that for the accumulation of CaO. A similar observation was made by McCarthy andc Metcalfe (1990).

4.9. Implications for the regional geomorphology and vegetation dynamics

It is well established that swamp abandonment due to channel avulsion is a regular occurrence in the Okavango Delta (Wilson, 1973; McCarthy et al., 1986a), and operates on a time scale of ~100 yr (McCarthy et al., 1988). As a channel system fails, the flanking swamp dries out and accumulated peat burns off (Ellery et al., 1989). After abandonment, the water table probably subsides and calcite and amorphous silica accumulation would cease. Complete leaching of accumulated soluble salts could now occur (McCarthy and Metcalfe, 1990), and islands would be effectively rehabilitated in terms of their ability to support vegetation. However, calcite and amorphous silica would remain behind in the soil because of their lower solubilities, although an increase in the density of the carbonate may occur as a result of local dissolution and precipitation induced by rainfall. During these periods bioturbation by termites would cause vertical redistribution of calcite, as termites selectively remove the finer soil particles (mainly calcite and amorphous silica) for the construction of termitaria (McCarthy et al., 1986b). This is most probably the reason why many of the islands show the occasional higher CaO zone at surface. In the short term an abandoned area may remain dry, or may become seasonally

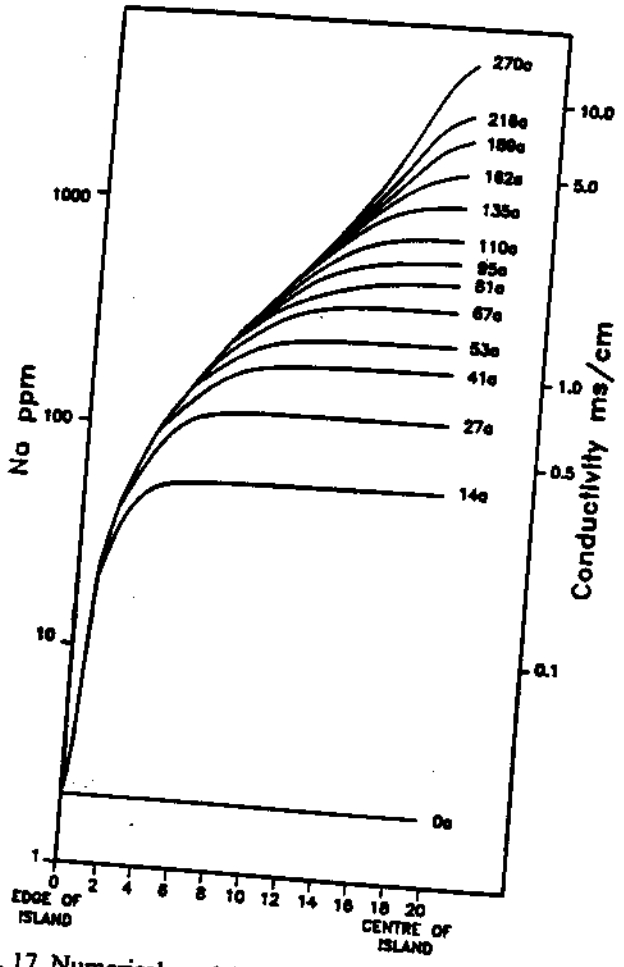

Fig. 17. Numerical model showing the development of the salinity profile in the groundwater beneath an island as a function of time. These curves are derived from model *8* in Fig. 14a.

flooded. However, once the area becomes perennially flooded again, a new cycle of Na accumulation would start and calcite and amorphous silica would again accumulate. The salinity of the groundwater therefore only reflects the current cycle of accumulation, while the CaO represents the aggregate of all previous cycles of inundation.

The above analysis of accumulation times of Ca suggests that islands are stable features on the landscape over periods measured in thousands to tens of thousands of years. Those with high CaO contents in the soils (e.g., island *F*) must be the oldest, while those with low CaO contents (e.g., island *E*) must be relatively young features.

In view of the probable great age of the islands, one might expect to see some evidence of erosion. Islands which have intermediate CaO contents in their soils (e.g., islands *A*, *B*, *C*) show good correspondence between shape of the isopleths and surface topography, but islands with high CaO (islands *D* and *F*), show truncation of the isopleths by the island surface. This does suggest some degree of erosion, although it must be remembered that the topographic gradients on all of these islands are very low, which is not conducive to erosion. Although limited, the amount of erosion may be sufficient to destroy any relationship between topographic height and maximum CaO (i.e. age) across a range of islands.

5. General discussion

Islands studied in this work appear to be of two distinct types — those in which topography is closely related to soil chemistry (all islands except *E*), and island *E* where no such relationship exists. These two groups of islands also differ in gross morphology. Island *E* is a long, sinuous feature and resembles an old channel in general shape (Fig. 18). It appears to have formed by topographic inversion following abandonment of a large, meandering channel system, as has been observed elsewhere in the Okavango Delta (McCarthy et al., 1988). In contrast, the other islands studied are smaller and irregular in form. In these islands, the degree of correspondence between CaO content of the soils and topography varies. Where maximum CaO is in the range 4–7%, correspondence is good, but deteriorates where soil CaO is very high. Since the CaO content is considered to be related to age, this deterioration probably reflects the greater age and hence more eroded condition of the high CaO islands.

Actual rates of accumulation of calcite and amorphous silica in the soil are difficult to estimate, because rates of evapotranspiration from islands are unknown. Assuming that these evapotranspirational rates are the same as the

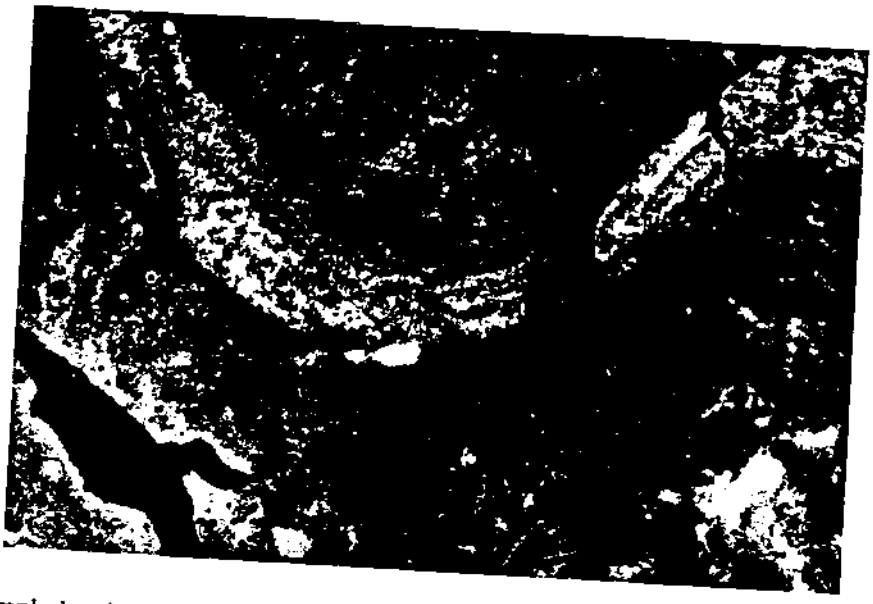

Fig. 18. Aerial photograph showing a portion of island *E*. The field of view is 2.7 km.

average for the entire Delta, the aggradation rate averaged over an entire island would be of the order of 3 cm kyr^{-1}. However, aggradation would only occur during periods of inundation and a large proportion of any 1-kyr period would be spent in a dormant condition when the area is abandoned, so that real aggradation rates would be much slower. This suggests that the islands are ancient features on the landscape of the Delta. Studies conducted in the vicinity of abandoned channels (McCarthy et al., 1988) reveal that an aggradational increment of the order of 30 cm may result during a single 100-yr inundation cycle. It is likely, therefore, that islands in areas close to channels may become submerged during channel induced aggradation (e.g., Wilson, 1973). However, in areas remote from channels, effective aggradation during each cycle of inundation is likely to be much less because of the very low ash content of peats which form in such areas (McCarthy et al., 1989), allowing islands to persist.

While this study has revealed a probable causal connection between calcite (and by inference, silica) precipitation and the topography of many islands, the question of the ultimate origin of these islands remains unresolved. It seems that the processes involved in calcite precipitation require an initial topographic irregularity upon which an island can nucleate. This irregularity provides a site above water level upon which woody species can survive local flooding. Once formed it is likely that this irregularity will perpetuate vertically as the fan aggrades. Topographic irregularities are constantly being created by termites during periods of swamp abandonment and it possible that these may constitute the nucleii of new islands. In addition, topographic irregularities formed initially by fluvial processes will in the long term also become sites of calcite and silica accumulation (e.g., island *E*) and will probably also evolve into calcite-enriched islands. Evidence to support this comes from the common occurrence of linear chains of islands.

6. Conclusions

This study has revealed that islands in the permanent swamps of the Okavango Delta are formed by the localized accumulation of silica and calcite, the precipitation of which induces

vertical expansion. The study has further revealed that woody plant species are active participants in island evolution and indeed appear to be the major cause of island growth.

From the analysis presented in this work, it is possible to reconstruct the evolutionary history of an island in the permanent swamps of the Okavango Delta. After initial inundation the island is well vegetated with a very diverse plant community. Transpiration, particularly by deep-rooted species lowers the water table beneath the island inducing inflow of water from the flanking swamp and from below. The water becomes progressively enriched in dissolved salts and the saturation points of silica and calcite are exceeded, causing precipitation of these constituents below the water table. This occurs centrally beneath small islands, but towards the edges of larger islands. Increasing salinity of the groundwater towards the centre of the island kills the less salt tolerant species but eventually all trees disappear. A steady-state concentration gradient around the edges of the islands maintains salinity at tolerable levels and ensures the survival of a diverse vegetation community on the island fringe. Capillarity draws the saline groundwater towards the surface in the centre of the island and evaporation deposits trona crusts. The resulting soil salinity kills the grass, producing a barren interior on the island. This stage of development is probably reached in a period of between 100 and 200 yr, during which time an increment of aggradation of the island surface has occurred as a result of the precipitation of calcite and silica in the subsurface. At any stage, the above process may be interrupted by swamp abandonment, during which accumulation of silica and calcite ceases and sodium salts are leached from the soils. Reflooding starts the process anew. Over hundreds of cycles of flooding and abandonment, the islands gradually aggrade as silica and calcite precipitate below the water table.

Island formation must be an important component of the aggradational processes which operate on the Okavango Delta fan and much of the estimated 300-m thickness of accumulated sediment probably consists of island-type deposits. Although the actual precipitation is by inorganic processes, plants clearly have played an important role. The importance of vegetation in regulating the fluvial processes which operate in the permanent swamps has been recognized (McCarthy et al., 1986a, 1988, 1989; Ellery et al., 1989). It now appears that aggradation on islands is also the result of plant growth. It is therefore clear that living organisms are intimately involved in, and perhaps completely control, the aggradational processes which operate in the permanent swamps.

Acknowledgements

The authors would like to thank: Mr. David Hartley and the staff of Okavango Explorations as well as Mr. A. Windram for providing logistical support for this study; Mr. Olivier Piton for his assistance in the field, Mrs. S. Hall and V. Govender for analytical assistance; Mrs. L. Whitfield for draughting and Ms. J. Wilmot for typing. Research funding was provided by the University of the Witwatersrand and the Jim & Gladys Taylor Trust.

References

Brown, S., 1981. A comparision of the structure, primary productivity and transpiration of cypress ecosystems in Florida. Ecol. Monogr., 51: 403–427.

Dinçer, T., Hutton, L.G. and Kupee, B.B.J., 1981. Study, using stable isotopes of flow distribution, surface-groundwater relations and evapotranspiration in the Okavango Swamp, Botswana. IAEA (Int. At. Energy Agency), Vienna, Proc. Ser. SII/AUB/493, pp. 3–26.

Ellery, W.N., Ellery, K., McCarthy, T.S., Cairncross, B. and Oelofse, R., 1989. A peat fire in the Okavango Delta and its importance as an ecosystem process. Afr. J. Ecol., 27: 7–21.

Eugster, H.P., 1980. Lake Magadi, Kenya, and its precursors. In: A. Nissenbaum (Editor), Hypersaline Brines and Evaporitic Environments. Developments in Sedimentology, 28. Elsevier, Amsterdam, pp. 195–232.

Eugster, H.P. and Jones, B.F., 1979. Behavior of major

solutes during closed-basin brine evolution. Am. J. Sci., 279: 609–631.

Garrels, R.M. and Mackenzie, F.T., 1967. Origin of the chemical composition of some springs and lakes. In: Equilibrium Concepts in Natural Water Systems. Am. Chem. Soc., Adv. Chem., 67: 222–242.

Hutchins, D.G., Hutton, S.M. and Jones, C.R., 1976. The geology of the Okavango Delta. Symp. on the Okavango Delta, Botswana Soc., Gaborone, pp. 13–20.

Hutton, L.G. and Dinçer, T., 1976. Chemistry and stable isotope composition of Okavango Delta waters. UNDP–FAO (U.N. Dev. Prog.–Food Agric. Org.), Gaborone, BOT/71/506, Tech. Note 23, 20 pp.

McCarthy, T.S. and Metcalfe, J., 1990. Chemical sedimentation in the semi-arid environment of the Okavango Delta, Botswana. Chem. Geol., 89: 157–178.

McCarthy, T.S., Ellery, W.N., Rogers, K.H., Cairncross, B. and Ellery, K., 1986a. The roles of sedimentation and plant growth in changing flow patterns in the Okavango Delta, Botswana. S. Afr. J. Sci., 82: 579–584.

McCarthy, T.S., McIver, J.R. and Cairncross, B., 1986b. Carbonate accumulation on islands in the Okavango Delta. S. Afr. J. Sci., 82: 588–591.

McCarthy, T.S., Stanistreet, I.G., Cairncross, B., Ellery, W.N. and Ellery, K., 1988. Incremental aggradation on the Okavango Delta-fan, Botswana. Geomorphology, 1: 267–278.

McCarthy, T.S., McIver, J.R., Cairncross, B., Ellery, W.N. and Ellery, K., 1989. The inorganic chemistry of peat from the Maunachira channel–swamp system, Okavango Delta, Botswana. Geochim. Cosmochim. Acta, 53: 1077–1089.

McCarthy, T.S., Stanistreet, I.G. and Cairncross, B., 1991a. The sedimentary dynamics of active fluvial channels on the Okavango fan, Botswana. Sedimentology, 38: 471–487.

McCarthy, T.S., McIver, J.R. and Verhagen, B.T., 1991b. Ground water evolution, chemical sedimentation and carbonate brine formation on an island in the Okavango Delta swamp, Botswana. Appl. Geochem., 6: 577–596.

Mueller-Dombois, D. and Ellenberg, H., 1974. Aims and Methods of Vegetation Ecology. Wiley, Toronto, Ont., 547 pp.

Norrish, K. and Hutton, J.T., 1969. An accurate X-ray spectrographic method for the analysis of a wide range of geological samples. Geochim. Cosmochim. Acta, 33: 431–453.

Scholtz, C.H., 1975. Seismicity, tectonic and seismic hazard of the Okavango Delta. UNDP–FAO (U.N. Dev. Prog.–Food Agric. Org.), Gaborone, Proj. Rep. BOT/71/506, 40 pp.

Shaw, P.A., 1984. A historical note on the outflow of the Okavango Delta system. Botswana Notes Rec., 16: 127–130.

UNDP (U.N. Development Programme), 1977. Investigation of the Okavango Delta as a primary water resource for Botswana. UNDP–FAO (U.N. Dev. Prog.–Food Agric. Org.), Gaborone, BOT/71/506, 361 pp.

Wilson, B.H., 1973. Some natural and man-made changes in the channels of the Okavango Delta. Botswana Notes Rec., 5: 132–153.